Canadian Solar Buildings Conference
Montreal, August 20-24, 2004
Refereed Paper

DEVELOPMENT OF A NEW SOLAR COLLECTOR MODEL IN ESP-R

Didier Thevenard[1], Kamel Haddad[2] and Julia Purdy[2]

[1]British Columbia Institute of Technology, Burnaby, BC
[2]CANMET Energy Technology Centre, Natural Resources Canada, Ottawa, ON

ABSTRACT

As part of an ongoing development to update the solar domestic hot water (SDHW) system simulation in the HOT3000 residential building energy analysis software, it was determined that a new solar collector model was required. The collector model currently available in the HOT3000 simulation engine ESP-r requires a significant number of inputs – inputs that would not be available to the typical user.

This paper describes the development of a new solar collector component model, to be used within a plant network to simulate SDHW systems in ESP-r. The model is based on empirical collector performance results and requires only a limited number of inputs. It is implemented as a set of separate subroutines that can be called by the ESP-r engine.

The paper details the inputs, outputs, and parameters of the model, as well as the equations that are used to calculate collector efficiency. The applicability of the model to both 'North-American' and 'European' types of efficiency equations is discussed. Modifications to the plant databases, integration within the ESP-r plant model, and coefficients for the sub-matrices that define the mass flow and energy balances on the solar collector's nodes are reviewed. Simulation results for a typical solar domestic hot water system are briefly presented.

INTRODUCTION

Background

The CANMET Energy Technology Centre (CETC) develops, distributes, and supports building simulation software for the Canadian construction industry. These software tools are used to optimize the energy performance of house and building designs as well as demonstrate compliance with energy rating programs such as EnerGuide for Houses[1] and performance-based compliance programs such as R-2000[2], and the Commercial Building Incentive Program[3].

One of CETC's principal software tools is HOT2000 (2003), a residential energy analysis program. HOT2000 has evolved over the past 20 years by incorporating more complex and detailed calculation methods. The software has been thoroughly validated, and its user-friendly interface is designed around the needs of practicing building professionals.

The engine of our next-generation versions of HOT2000, coined ESP-r/HOT3000 (Haltrecht et al. 1997 and ESRU 2000), incorporates a time-step simulation, as well as many models of interest to the building industry. Some of these models include a residential fuel cell model and a comprehensive air-to-air heat recovery (HRV) model.

---

[1] An energy-efficiency rating programme that offers to help homeowners make home retrofit choices that improve the comfort and energy efficiency of their homes. Independent energy advisors visit the home to identify how the house uses energy and where it is being wasted.

http://oee.nrcan.gc.ca/houses-maisons/

[2] A housing programme that encourages the building of energy-efficient houses that are both environmentally friendly and healthy to live in. http://oee.nrcan.gc.ca/r-2000/

[3] CBIP offers a financial incentive to encourage building owners to reduce energy consumption of their buildings to 25% less than the Model National Energy Code for Buildings. http://oee.nrcan.gc.ca/newbuildings/

Objective

The objective of this project was to develop a solar collector model that can be used with ESP-r's plant and systems network. The collector model currently available in the ESP-r engine requires a significant number of inputs which are often too arcane for the the typical user, such as the absorber plate emittance or the collector fin efficiency factor. By comparison, the new model is based on empirical collector performance results and requires only a limited number of inputs.

The model does not intend to replace specialized programs such as WATSUN, a computer program developed in the 1980s at the University of Waterloo for the hourly simulation of solar energy systems; rather, it aims at bringing into ESP-r some of the modeling capabilities and algorithms used in such programs, to enable the *integrated* simulation of residential buildings and solar energy systems.

MODEL ALGORITHM

The basic formulation is relatively straightforward, as long as collector efficiency is expressed as a function of collector outlet temperature. We start with this formulation, then show how it can be adapted to include other types of efficiency equations, and modified to include flowrate and incidence angle effects; a discussion of collector thermal mass and the calculation of coefficients for the sub-matrices that define the energy balance on the solar collector's nodes are then reviewed.

Basic formulation

To use the same formulation as other ESP-r plant components, the collector is modeled as a one-node component, shown in Figure 1. The node essentially represents the outlet temperature of the collector. The collector is characterized by its efficiency, defined as the ratio of energy harvested over a specified time period to the amount of solar radiation incident upon the collector over the same period. To obtain equations that best fit the formalism of ESP-r, collector efficiency is then expressed as a function of outlet temperature:

$$\eta = \eta_{0,out} - \eta_{1,out} \frac{(\theta_{out} - \theta_e)}{G} \quad (1)$$

where $\eta_{0,out}$ and $\eta_{1,out}$ are two parameters characteristic of the collector, θ_{out} is the collector outlet temperature, θ_e is the temperature of the environment (ambient temperature) and G is the solar radiation incident upon the collector. An energy balance on the collecor leads to:

$$M\overline{c}\frac{\partial \theta_{out}}{\partial t} = -\dot{m}C_p(\theta_{out} - \theta_{in}) + \eta AG \quad (2)$$

where M is the mass of the collector and the fluid it contains, $\overline{c}$ is the collector mass weighted average specific heat capacity, $\dot{m}$ is the flowrate through the collector, θ_{in} is the collector inlet temperature, and A is the gross area of the collector. This equation is not correct in the sense that the left-hand side should use some 'average' collector temperature to represent the energy stored within the collector. Here, we assume that all the mass of the collector is concentrated at the collector's exit. Similar assumptions are made for other components in ESP, probably to simplify the structure of the solution matrix; for example the flow conduit component (see section 5.4.5 of Hensen, 1991) uses the same hypothesis. In any case the validity of this hypothesis will not matter since, as will be seen, the time-dependent term will later be dropped from the equation.

Combining equations (1) and (2), and identifying θ_{out} with the component's node temperature θ_k, and that θ_{in} with the node temperature θ_j of the component j which feeds into the collector (see Figure 1), one can rewrite the equation as:

$$\begin{aligned} M\overline{c}\frac{\partial \theta_k}{\partial t} &= -\dot{m}C_p(\theta_k - \theta_j) \\ &\quad + \eta_{0,out}AG - \eta_{1,out}A(\theta_k - \theta_e) \end{aligned} \quad (3)$$

This equation is essentially in the form of equation 5.1 of Hensen (1991) and is therefore ready to be programmed into ESP-r.

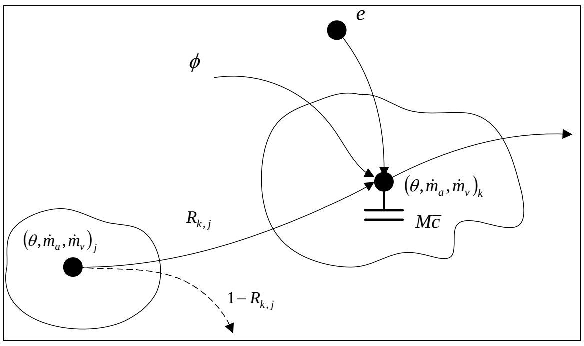

Figure 1. The collector model.

Use of collector efficiency equations based on inlet or average temperatures

However, collector efficiencies are rarely reported as a function of outlet temperature, as used by equation (1). North-American test results generally use the inlet temperature, whereas European test results are often reported in terms of average collector temperature. Furthermore, test reports generally provide a quadratic equation:

$$\eta = \eta_0 - \eta_1 \frac{\Delta\theta}{G} - \eta_2 \frac{\Delta\theta^2}{G} \tag{4}$$

where $\Delta\theta$ is defined by:

$$\Delta\theta = \theta_{in} - \theta_e$$

(North-American efficiency equation)

$$\Delta\theta = \theta_{avg} - \theta_e$$

(European efficiency equation)

with θ_{avg} the average of collector inlet and outlet temperatures $\theta_{avg} = (\theta_{in} + \theta_{out})/2$. It is therefore necessary to convert equations in form (4) to equations in form (1). The method is explained first in the case of a linear collector ($\eta_2 = 0$ in equation 4), then in the case of a quadratic collector.

<u>Linear collector efficiency equation</u>

The collector's energy balance equation, expressing the collector efficiency as a function of the inlet temperature, is written as:

$$M\overline{c}\frac{\partial\theta_{out}}{\partial t} = -\dot{m}C_p(\theta_{out} - \theta_{in}) + \eta_{0,in}AG - \eta_{1,in}A(\theta_{in} - \theta_e) \tag{5}$$

where $\eta_{0,in}$ and $\eta_{1,in}$ are the coefficients of the efficiency equation expressed as a function of the collector inlet temperature. Rewriting the last term as:

$$(\theta_{in} - \theta_e) = (\theta_{in} - \theta_{out}) + (\theta_{out} - \theta_e) \tag{6}$$

then equation (5) can be rearranged into:

$$M\overline{c}\frac{\partial\theta_{out}}{\partial t} = -(\dot{m}C_p - A\eta_{1,in})(\theta_{out} - \theta_{in}) + \eta_{0,in}AG - \eta_{1,in}A(\theta_{out} - \theta_e) \tag{7}$$

This is equivalent to equation (3) in which $\dot{m}C_p$ is replaced with $(\dot{m}C_p - A\eta_{1,in})$, and $\eta_{0,out}$ and $\eta_{1,out}$ are replaced with $\eta_{0,in}$ and $\eta_{1,in}$.

A similar development (which the reader is spared) is used to provide an equivalence with efficiency equation based on average collector temperature. In that case, equation (3) may be used again, provided $\dot{m}C_p$ is replaced with $(\dot{m}C_p - A\eta_{1,avg}/2)$, and $\eta_{0,out}$ and $\eta_{1,out}$ are replaced with $\eta_{0,avg}$ and $\eta_{1,avg}$, the coefficients of the efficiency equation expressed as a function of the collector averate temperature. This leads to the following equation:

$$M\overline{c}\frac{\partial\theta_{out}}{\partial t} = -\left(\dot{m}C_p - \frac{A\eta_{1,avg}}{2}\right)(\theta_{out} - \theta_{in}) + \eta_{0,avg}AG - \eta_{1,avg}A(\theta_{out} - \theta_e) \tag{8}$$

<u>Quadratic collector efficiency equation</u>

If a quadratic collector efficiency equation is used ($\eta_2 \neq 0$ in equation 2), the formulae above cannot be used. Following the approach used in TRNSYS (2004), the equation is linearized as:

$$\eta = \eta_0 - (\eta_1 + \eta_2\Delta\theta)\frac{\Delta\theta}{G} \tag{9}$$

In that equation, $\Delta\theta$ represents the temperature differential $\theta_{in} - \theta_e$ or $\theta_{avg} - \theta_e$, depending on the type of efficiency equation considered. The non-linear nature of equation (9) requires special consideration. The convention in ESP-r is to linearize non-linear terms by evaluating coefficients using the previous time-row's solution. This approach is suitable for the simulation of components that have a large time constant. In the case of solar collectors the time constant is small – the collector response is usually much smaller than the time step, which is often between 10 minutes and one hour – and this approach could lead to siginificant errors in the estimation of energy collected. For that reason, the non-linear nature of equation (9) requires that ESP-r iterates to find $\Delta\theta$.

Correction for flowrate

If the flowrate at which the collector is used is different from the one at which it was tested, the efficiency is slightly modified. The correction algorithm is detailed in section 6.20 of Duffie and Beckman (1991) and its derivation is not repeated here. The end result of the calculation is that the efficiency needs to be multiplied by a coefficient r defined as:

$$r = \frac{B_u}{B_t}\frac{[1 - \exp(-1/B_u)]}{[1 - \exp(-1/B_t)]} \tag{10}$$

where B_u and B_t are defined as:

$$B_t = \frac{\dot{m}_t C_{p,t}}{AF'U_L} \tag{11}$$

$$B_u = \frac{\dot{m}_u C_{p,u}}{AF'U_L} \tag{12}$$

In equations (11) and (12), $\dot{m}$ represents the flow rate and C_p the collector fluid heat capacitance. Subscripts *t* and *u* refer respectively to the test and use conditions. $F'U_L$ is defined by:

$$F'U_L = -\frac{\dot{m}_t C_{p,t}}{A} \ln\left(1 - \frac{\eta_{1,in} A}{\dot{m}_t C_{p,t}}\right) \quad (13)$$

Note that this last equation requires the knowledge of $\eta_{1,in}$. If the efficiency equation is known based on average collector temperature, the following equation (Duffie and Beckman, 1991, section 6.19) is used:

$$\eta_{1,in} = \frac{\eta_{1,out}}{1 + \frac{A\eta_{1,avg}}{2\dot{m}C_p}} \quad (14)$$

Caution should be exercised when using flowrate corrections. The formulae above are known to work well in many configurations, but they do not always give a very accurate prediction of the actual change in efficiency, particularly when the change in flow rate results in a transition between laminar and turbulent flow in the collector tubes. This is a limitation of the model that cannot be avoided, the only way around it being to perform a full, detailed simulation of thermal exchanges in the collector.

Determination of the mass of the collector

The mass M of the collector and the water it contains, and its mass weighted average specific heat capacity $\bar{c}$ are often not known, which makes their use in equation (3) problematic. A solution that can be proposed is to let the user specify the time constant τ of the collector. According to equation (3) this time constant can be approximated by:

$$\tau = \frac{M\bar{c}}{\dot{m}C_p} \quad (15)$$

Knowing τ, this gives an estimate of $M\bar{c}$ which can be used in the model. However taking transient collector effects into consideration is too refined for most applications. Indeed, most collectors have a time constant in the order of 90 s, which is much smaller than the typical time step (15 mn) used for plant simulation. It is therefore legitimate to set $M = 0$ in equation (3) and to treat the problem as a quasi steady-state one.

Effects of the angle of incidence

The effects of the angle of incidence of the incoming radiation on the collector performance is usually accounted for (see Duffie and Beckman, 1991, ch. 6.17) through the use of an *incidence angle modifier* κ which is applicable to the radiation incident upon the collector. In other words, equation (3) becomes:

$$M\bar{c}\frac{\partial\theta_k}{\partial t} = -\dot{m}C_p(\theta_k - \theta_j) + \eta_{0,out}A\kappa G - \eta_{1,out}A(\theta_k - \theta_e) \quad (16)$$

A method used by many tests is to provide the following functional fit for κ:

$$\kappa = 1 - b_0\left(\frac{1}{\cos\zeta} - 1\right) - b_1\left(\frac{1}{\cos\zeta} - 1\right)^2 \quad (17)$$

where b_0 and b_1 are two parameters characteristic of the collector and ζ is the angle of incidence of solar radiation upon the collector. This is the formulation used in the current implementation of the model, although it should be noted that it is not without danger. First, there are some collectors for which the fit (16) proves unsatisfactory, particularly for angles of incidence greater than 45 or 60°; secondly, equation (16) can be ill-behaved when ζ becomes close to $\pi/2$, therefore it is necessary to add safeguards to prevent divide-by-zero or negative values of κ.

A second method which will be implemented shortly in ESP-r, for dealing with effect of incidence angle, is to allow the user to enter data pairs of incidence angle and an associated correction factor κ. An algorithm is then implemented that finds the two angle of incidences entered by the user that bound the actual angle of incidence during the time step. Then linear interpolation is used find the applicable correction factor.

Further refinements to the current incidence angle modification methods could include, as is done in TRNSYS (2004):

- applying the incidence angle modifier separately (and with different values of the incidence angle) to the direct, beam and reflected components of irradiance; and
- using different incidence angle modifiers in the vertical and horizontal directions (for anisotropic collectors).

Implementation of Capability to Model Water-Propylene Glycol Mixtures

The ESP-r plant domain was originally set up to model networks that use either water or moist air as the working fluid. For solar DHW systems it is common practice to use a mixture of water and propylene glycol in the collector loop to prevent freezing in cold climates. A new method then is needed to be able to simulate water-glycol mixtures in ESP-r.

A new input to the collector can then be implemented to specify the propylene glycol mass fraction in the fluid mixture. This input is then used in the solar collector subroutine to determine the proper physical properties to be used for the energy balance. The mass balance section of the subroutine sets the water and the propylene glycol flow rates to the appropriate values.

The algorithms of other plant componenets that can be connected to the solar collector, such as pumps, are then modified to verify whether there is an incoming propylene glycol flow imposed by the collector. Then the mass fraction of the propylene glycol mixed with the water is determined and then used to set the proper physical properties for the energy balance.

Summary of algorithm

The calculation algorithm can now be summarized:

1. Calculate the angle of incidence of direct beam solar radiation upon the collector.
2. Calculate the solar radiation in the plane of the collector.
3. Calculate the incidence angle modifier using equation (17).
4. Linearize the quadratic collector efficiency equation using (9).
5. Calculate the flowrate correction *r* using equations (10) to (13).
6. Modify the heat capacitance flowrate to account for the fact that the efficiency equation is not expressed as a function of the outlet temperature, using equations (7) or (8).
7. Use equation (3), modified with (10) and (17), to contribute to the ESP-r energy balance matrix, using equation 5.4 from Hensen (1991).

The model requires only 11 parameters to be entered by the user. A screenshot is shown in Figure 2.

a Collector area (m2)	:	2.8650
b Type of efficiency equation (1=North-American,2=Eu	:	1.0000
c Constant coef. of efficiency equ. (-)	:	0.70500
d Linear coef. of efficiency equ. (W/m2/C)	:	3.7240
e Quadratic coef. of efficiency equ. (W/m2/C2)	:	0.20000
f Collector test flow rate (kg/s)	:	0.20000E-01
g Heat capacitance of fluid used for test (J/kg/C)	:	4200.0
h Coefficient of linear term of IAM (-)	:	0.20000
i Coefficient of quadratic term of IAM (-)	:	0.0000
j Collector slope (deg. from horizontal)	:	45.000
k Collector azimuth (deg., N=0, E=90)	:	180.00

Figure 2. Parameters of the collector model.

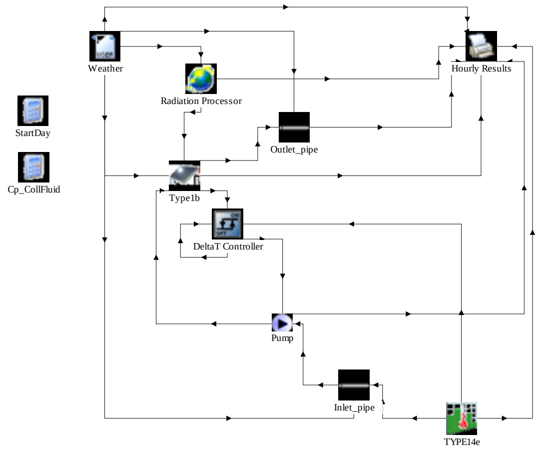

Figure 3. TRNSYS model used for test.

TEST AND EXAMPLE

The newly developed collector model was tested extensively. Manual checks were performed to verify the results of the calculations for the collector considered individually. The model was then tested as part of an entire system, and the results of a 6-month-long, full-system simulation were compared to those of a TRNSYS simulation for a similar system.

The model (see Figure 3 for the TRNSYS equivalent) represents an industrial process heat system with constant, 10 °C water feeding an inlet pipe which is connected to a pump. The pump is connected to the solar collector, whose output is directed to an outlet pipe. A controller turns the pump on and off according to the temperature of the collector outlet.

Collector parameters that were used in the model are those of Figure 2. Parameters for inlet and outlet pipes can be found in Figure 4, and pump parameters in Figure 5. The pump flow rate is set to 0.03 kg/s. The on/off controller turns the pump on if the plate temperature is greater than 60 °C, and turns it off if it falls below 12 °C (the TRNSYS model uses a equivalent differential temperature controller; the pump is turned on only if the temperature differential between the collector and the inlet pipe is greater than 50 °C, and is turned off when it becomes lower than 2 °C).

a Component total mass (kg)	:	2.0000
b Mass weighted average specific heat (J/kgK)	:	2250.0
c UA modulus from wall to environment (W/K)	:	2.0000
d Hydraulic diameter of pipe (m)	:	0.15000E-01
e Length of pipe section (m)	:	5.0000
f Cross sectional face area (m^2)	:	0.17670E-03

Figure 4. ESP-r parameters for inlet and outlet pipes.

```
a Component total mass (kg)                          :   5.0000
b Mass weighted average specific heat (J/kgK)        :   2250.0
c UA modulus from wall to environment (W/K)          :  0.20000
d Rated total absorbed power (W)                     :   20.000
e Rated volume flow rate (m^3/s)                     :  0.30000E-04
f Overall efficiency (-)                             :  0.70000
```

Figure 5. ESP-r parameters for the pump.

The simulation was run from April 1 to September 30 with weather data for Ottawa, ON. A 1-hour time step was used for the building and a 15-minute time step was used for the plant.

A direct comparison between TRNSYS and ESP-r is not an easy task. Both models have their peculiarities and subtleties, which can sometimes induce significant differences in the results. For example in one of our earlier simulations, the building model in ESP-r was run with hourly time steps and the plant model with quarter-hourly ones. It turned out that when the model is run that way, solar radiation on the collector was calculated only once per hour and the same value was used for all plant quarterly-hour time steps within that hour. TRNSYS, on the other hand, used quarter-hour time steps for solar radiation calculation. The different methods of calculating solar radiation then introduced artificial differences in the estimation of energy collected. We therefore learned that it was preferable, for comparison purposes, to run the ESP-r building model itself with a quarter-hourly time step. Even so, the comparison results presented in this paper can be considered as preliminary and may be refined as our simulations with both programs get better tuned.

	Incident radiation		
Month	TRNSYS (MJ)	ESP-r (MJ)	Difference (%)
April	1554	1562	0.5
May	1664	1683	1.1
June	1680	1702	1.3
July	1758	1782	1.4
August	1594	1606	0.8
September	1424	1416	-0.6
Total	**9674**	**9751**	**0.8**

Table 1. Comparison of TRNSYS and ESP-r solar radiation calculation.

Calculation of solar radiation

A plot of quarter-hourly solar radiation values calculated by ESP-r, vs. those calculated by TRNSYS, is shown in Figure 6. There is a small dispersion in the values calculated by the two programs. Looking at an individual day, for example May 24 (hours 3432-3456 in the simulation) as shown in Figure 7, one can reasonably infer that the dissimilarities are due to difference in the interpolation algorithm or the radiation algorithms used. However, as shown in Table 1, the differences are rather small (1.4% or less) on a monthly basis.

Calculation of energy collected

A plot of quarter-hourly values of energy collected calculated by ESP-r, vs. those calculated by TRNSYS, is shown in Figure 8. Although most values fall on the 1:1 line, there are a number of time steps for which ESP-r predicts collection whereas TRNSYS predicts none, as visible from the large concentration of points located on the Y-axis (there are also time steps for which TRNSYS predicts collection when ESP-r predicts none, as visible from the cluster of points on the X-axis; however these points are fewer in number and represent a lower amount of energy). As a consequence, ESP-r predicts more energy collected than TRNSYS, as is summarized on a monthly basis in Table 2. Over the simulation period, the overestimation is 14.6%, which is somewhat on the high side of what could be expected, and requires further explanation.

	Energy collected		
Month	TRNSYS (MJ)	ESP-r (MJ)	Difference (%)
April	311	366	17.6
May	537	633	17.8
June	662	759	14.7
July	748	830	11.0
August	720	801	11.2
September	464	557	20.1
Total	**3441**	**3945**	**14.6**

Table 2. Comparison of TRNSYS and ESP-r energy collected calculation.

Excluding those hours where one of the programs predicts collection and the other one doesn't, the comparison between ESP-r and TRNSYS becomes more favorable, as can be seen in the left part of Table 3.

Comparing Tables 2 and 3, one can see that most of the difference between ESP-r and TRNSYS results comes from hours where ESP-r predicts collection whereas TRNSYS doesn't. Such occurrences may happen either for legitimate reasons (i.e. as the solar incident radiation estimated by ESP-r is slightly higher than that calculated by TRNSYS, the collector will more easily reach the temperature threshold that will turn the pump on), or because the plate stagnation temperature is calculated differently in both programs, or because the control algorithm in ESP-r turns the pump on 'too soon'. This is still under investigation. The comparison of energy collected during an individual day (May 24, as before) is shown in Figure 9, which clearly illustrates the fact that ESP-r predicts the collection to start earlier than TRNSYS.

Table 3 also compares the results of simulations when the effect of incidence angle are removed (for the simulation results shown in the right part of Table 3, the incidence angle modifier were kept constant and equal to 1 by setting both coefficients in the incidence angle modifier equation to zero). This further analysis reveals that about half the dissimilarity between the results of the two programs (when considering only hours where both programs predict collection) comes from different calculation methods for angle of incidence effects, the method used in TRNSYS being more complicated than the one used in ESP-r.

CONCLUSION

A simplified solar collector model was implemented in ESP-r's plant model. The model requires a limited number of inputs that are widely available to users, and enables the inclusion of active solar systems in plant models.

Preliminary program-to-program comparisons with results from TRNSYS, a well-known program for the simulation of solar energy systems, show that the new collector model performs well. ESP-r's predictions tend to be a few percent higher than those of TRNSYS, when one limits the comparison to those hours where both programs predict collection. However ESP-r predicts collection more often than TRNSYS, and this leads ESP-r to overestimate energy collected by a somewhat larger amount (10 to 20% on a monthly basis) when all hours are taken into account. The reasons why the control algorithms turn the pump on differently in TRNSYS and ESP-r is still under investigation.

ACKNOWLEDGMENTS

Funding for this work was provided by CETC-Ottawa of NRCan's Energy Technology and Program Sector (ETPS).

REFERENCES

Duffie JA and Beckman WA (1991) Solar Engineering of Thermal Processes. John Wiley & Sons.

ESRU (2000), The ESP-r System for Building Energy Simulations: User Guide Version 9 Series, ESRU Manual U00/1, University of Strathclyde, Glasgow UK.

ESRU (2003), 'Tutorial on using IPV definition to scale models', Energy Systems Research Unit, University of Strathclyde, Glasgow, Scotland.

Haltrecht D., Zmeureanu R., and Beausoleil-Morrison I. (1999), 'Defining the Methodology for the Next-Generation HOT2000 Simulator', Proc. Building Simulation `99, (1) 61-68, International Building Performance Simulation Association, Kyoto Japan.

Hensen JLM (1991) On the thermal interaction of building structure and heating and ventilating system. PhD Thesis, Technische Universiteit Eindhoven.

HOT2000: A Comprehensive Tool for the Design of Energy Efficient Homes and Buildings, Version 9.1, Natural Resources Canada, 2003. www.buildingsgroup.nrcan.gc.ca/software/hot2000_e.html

TRNSYS (2004) User's manual – Volume 5, mathematical reference. Solar Energy Laboratory, University of Wisconsin-Madison.

	Energy collected (complete model)			Energy collected (without incidence angle modifiers)		
Month	TRNSYS (MJ)	ESP-r (MJ)	Difference (%)	TRNSYS (MJ)	ESP-r (MJ)	Difference (%)
April	310	312	0.8	355	356	0.4
May	534	543	1.7	675	686	1.6
June	656	676	3.1	817	834	2.0
July	742	768	3.5	892	908	1.8
August	718	737	2.7	841	849	1.0
September	463	468	0.9	568	566	-0.3
Total	**3423**	**3504**	**2.4**	**4146.2**	**4198**	**1.3**

Table 3. Comparison of TRNSYS and ESP-r energy collected calculation, only for hours where both programs predict collection.

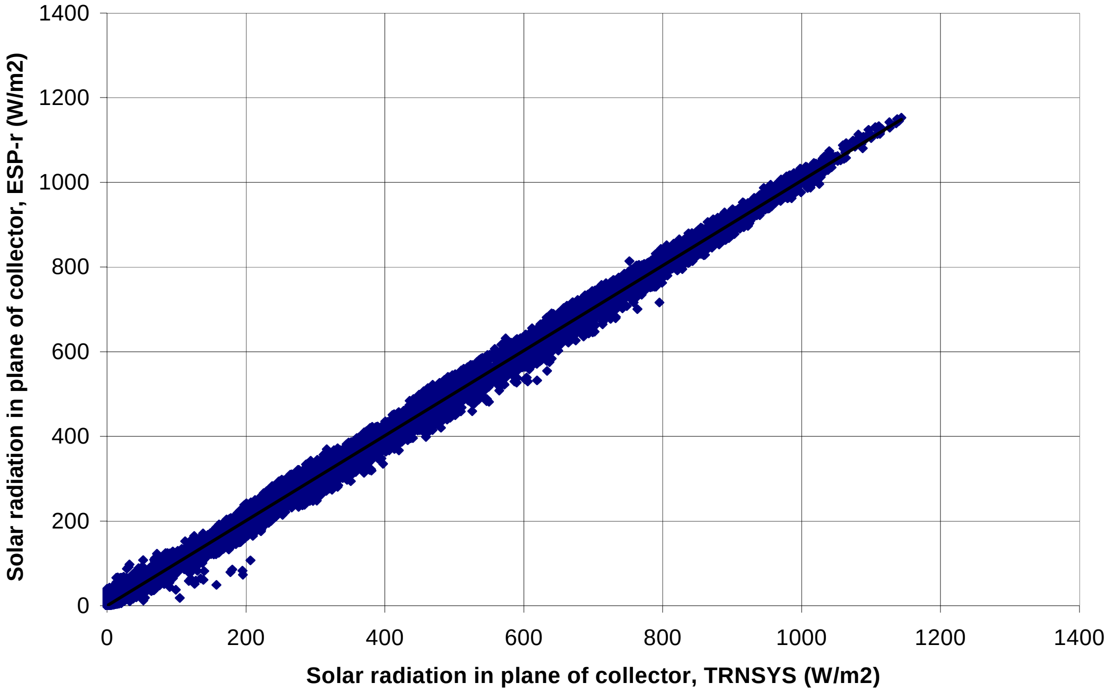

Figure 6. Comparison of solar radiation calculated by ESP-r and TRNSYS.

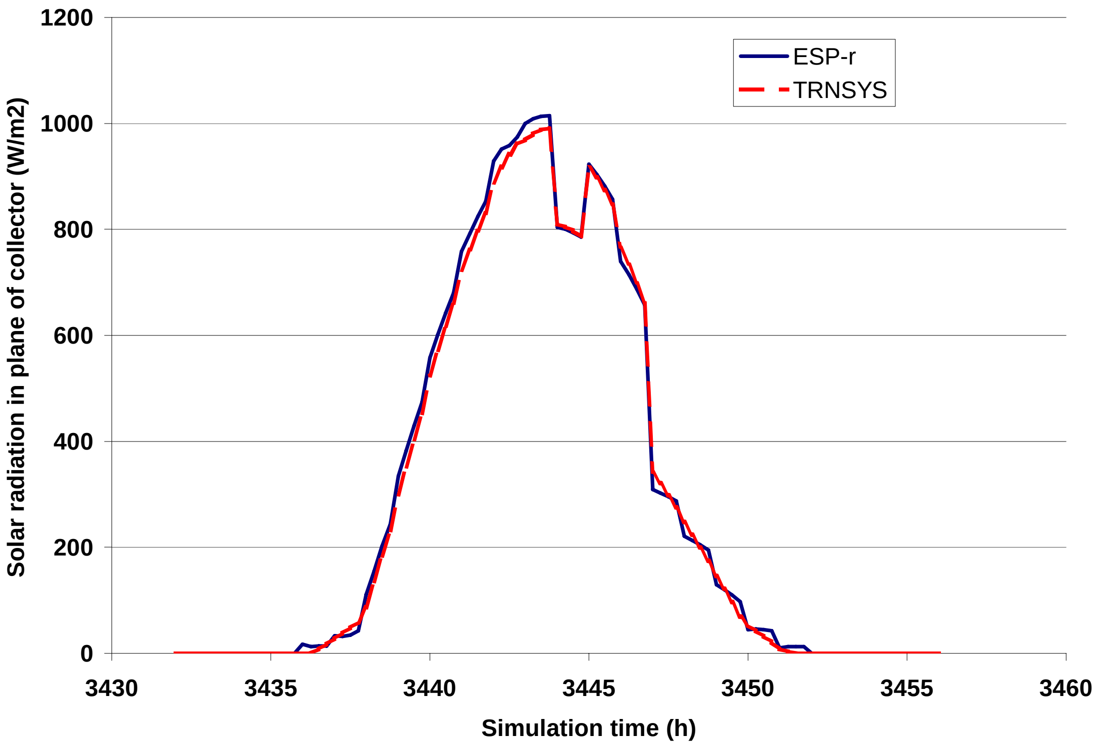

Figure 7. Comparison of solar radiation calculated by ESP-r and TRNSYS for May 24.

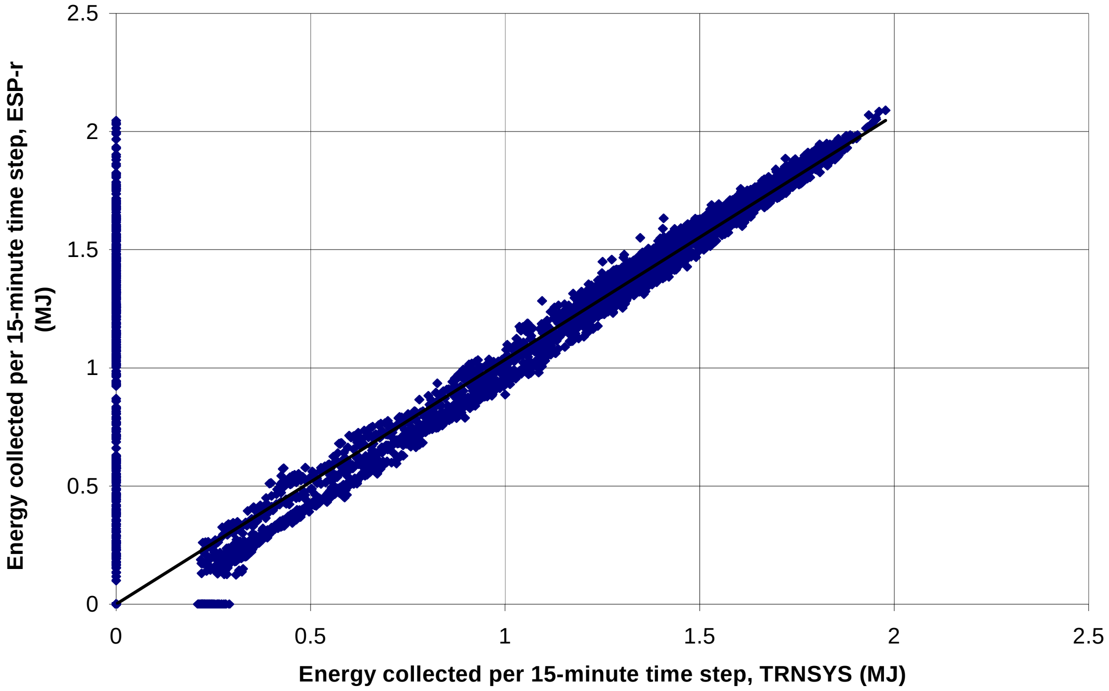

Figure 8. Comparison of energy collection calculated by ESP-r and TRNSYS.

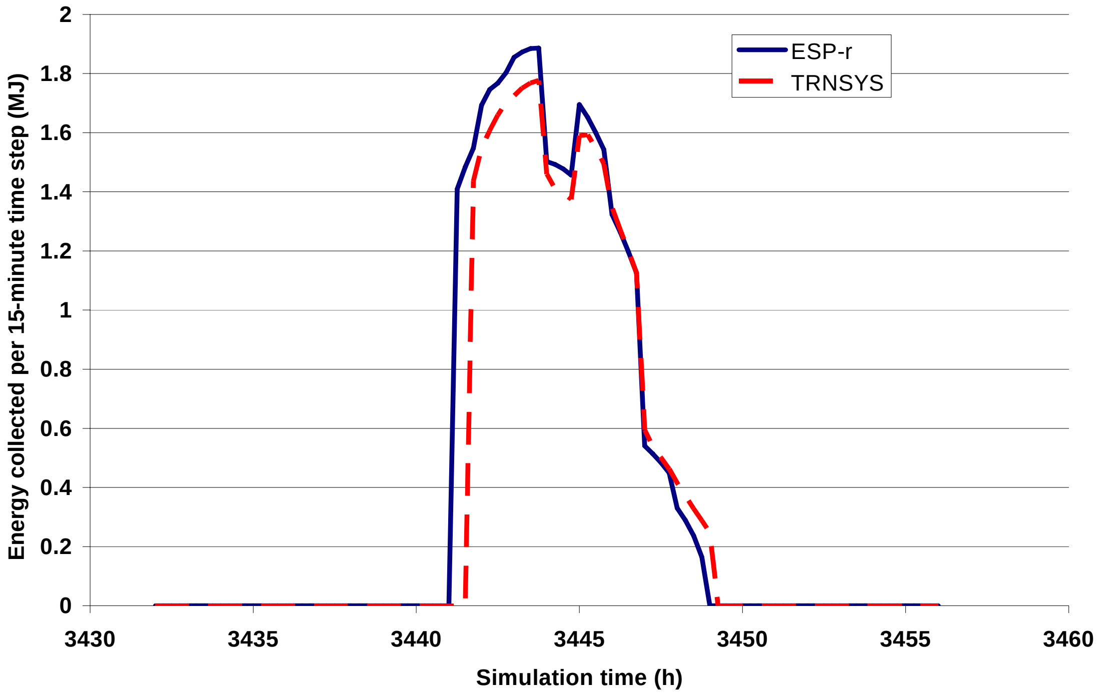

Figure 9. Comparison of energy collection calculated by ESP-r and TRNSYS for May 24.